Optimized Intermolecular Potential for Aromatic Hydrocarbons Based on Anisotropic United Atoms. 1. Benzene

R. Oliver Contreras-Camacho,[†,‡] Philippe Ungerer,[§,||] Anne Boutin,[§] and Allan D. Mackie*[,†]

Departament d'Enginyeria Química, ETSEQ, Universitat Rovira i Virgili, Avinguda dels Països Catalans 26, Campus Sescelades, 43007 Tarragona, Spain, Laboratoire de Chimie Physique, Université de Paris Sud, Bâtiment 349, 91405 Orsay Cedex, France, and Institut Français du Pétrole, 1-4 Avenue de Bois Préau, 92852 Rueil-Malmaison, Cedex, France

Received: March 24, 2004; In Final Form: June 28, 2004

An optimization has been performed for the parameters of an Anisotropic United Atoms intermolecular potential for benzene for thermodynamic property prediction using Gibbs Ensemble and NPT Monte Carlo simulations. The optimization procedure is based on the minimization of a dimensionless error criterion incorporating various thermodynamic data (saturation pressure, vaporization enthalpy, and liquid density) at ambient conditions and at 450 K. A comprehensive comparison of the new model is given with six intermolecular potentials taken from the literature. Overall, thermodynamic property estimations of our optimized model are in very good agreement with experimental data. The new model also provides a good representation of the liquid structure, as revealed by the carbon−carbon radial distribution function.

1. Introduction

Since molecular simulation presents the advantage of providing a unified theoretical framework for modeling the thermodynamic properties of fluids, over the last few decades a variety of force fields have been proposed for organic systems.[1−15] However, there is still a strong need for improved intermolecular potential energy models capable of predicting the equilibrium properties of a large variety of organic compounds over a wide range of temperatures. Over the past decade, the Anisotropic United Atoms (AUA) approach initiated by Toxvaerd[16,17] has been proposed as an efficient way to provide more accurate intermolecular potentials without significantly increasing computer time requirements, as compared with more conventional United Atoms (UA) potentials.[18−24] The purpose of the present work is to investigate the capability of the AUA potential to model the benzene molecule as a preliminary step before other aromatic molecules can be considered.

Computer simulation studies of benzene have in general focused on its solid and liquid structural features, dynamics, vibrational spectra, structure of the dimer, trimer or tetramer conformations, and the related energies.[10,15,25−34] Many of these studies have proposed new force fields. Among these models, the use of a single Lennard−Jones center located in an intermediate position between the carbon and the hydrogen centers was proposed as early as 1976 by Evans and Watts[28] to model the second virial coefficient and the solid-phase structure of benzene. This type of model was further explored by Friedrich and Lustig[29,35] to represent the vapor−liquid equilibrium of benzene. Meanwhile, other models considered a classical UA approach where the force center is located on the carbon center, either using the Lennard−Jones potential[10,27,32] or an exponential-6 potential.[15] All Atoms (AA) models including electrostatic charges were also proposed based on the structural and liquid properties of the liquid phase.[5,30] In the present work, we apply these models in order to test their capability to reproduce phase behavior properties and compare them to a new AUA model.

The new AUA model of benzene developed in the present work is based on a Lennard−Jones force center for the CH group located between the carbon and the bonded hydrogen (Figure 1), in the same way as the models of Evans and Watts[28] and Friedrich and Lustig.[29] The determination of the Lennard−Jones parameters and the position of the force center is based on the minimization of a dimensionless error criterion incorporating various thermodynamic data (saturation pressure, vaporization enthalpy, and liquid density), following the same approach as previous AUA parameter optimizations.[18]

This paper is organized as follows. We give first a brief description of the simulation methods used to compute both thermodynamic properties and parameter optimization. In a subsequent section, we detail the force field development for the CH group of benzene. We then compare the new AUA potential with several of the preexisting models[10,15,27−30,32] on the basis of coexistence densities, vapor pressures, and enthalpies of vaporization along the coexistence curve. Finally, we investigate the liquid structure of pure benzene at room conditions with the same potentials.

2. Simulation Methods

2.1. Potential Energy Models. With the exception of the exponential-6 potential,[15] the effective dispersion−repulsion interactions between two atoms or united atoms (*i* and *j*) of different molecules are represented by the Lennard−Jones 6-12 equation:

$$U^{i,j}(r_{ij}) = 4\epsilon_{ij}\left[\left(\frac{\sigma_{ij}}{r_{ij}}\right)^{12} - \left(\frac{\sigma_{ij}}{r_{ij}}\right)^{6}\right] \quad (1)$$

In the case of the OPLS All Atoms (OPLS-AA) potential,[30] the electrostatic energy is obtained by summing the pairwise Coulombic interactions between the partial charges belonging

* Corresponding author e-mail: amackie@etseq.urv.es.
† Universitat Rovira i Virgili.
‡ Presently at Institut Français du Pétrole.
§ Université de Paris Sud.
|| Institut Français du Pétrole.

10.1021/jp048693j CCC: $27.50
Published on Web 08/19/2004

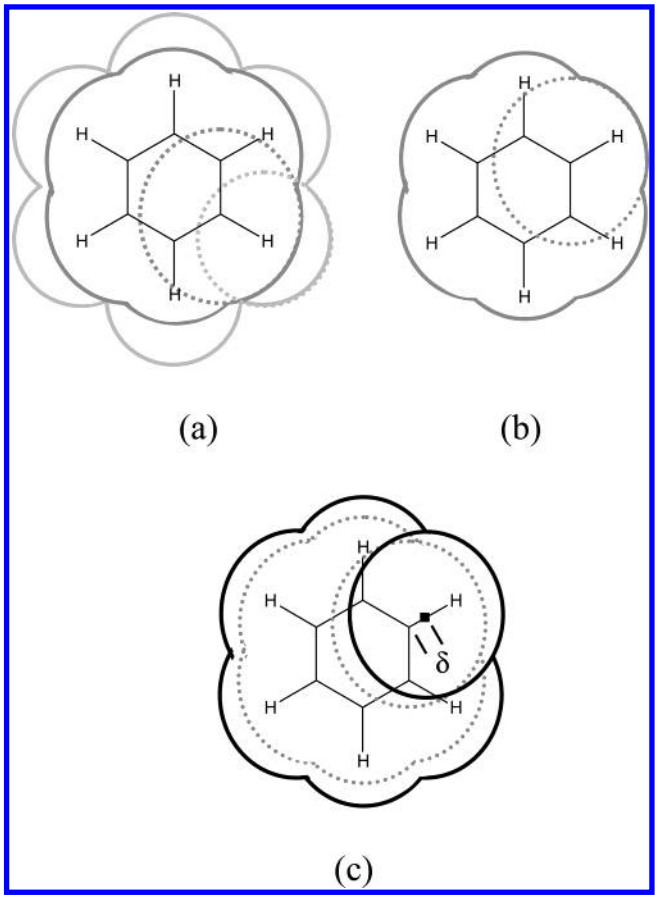

Figure 1. Schematic representation of benzene models used in molecular simulation. (a) All-Atoms model (AA), each carbon and hydrogen atom is represented as an individual interaction site. (b) Six-sites model representation, also known as United Atoms (UA), each interaction site corresponds to one CH group. (c) Anisotropic United Atoms (AUA) representation, the exclusion sphere of the CH group in the UA model (dotted line) compared with the displaced exclusion spheres of the AUA model (solid lines). δ is the displacement of the force center of the group. These views are taken perpendicular to the plane containing the carbon and the hydrogen atoms of the group.

to the different molecules. Since the electrostatic contribution to the OPLS model represents a maximum of 7% to the total intermolecular energy, we have decided to not consider this contribution into the development of new model. No polarization energy is taken into account in the potential energy models considered in this study. Since the benzene molecule is assumed to be rigid, no stretching, bending, or torsional energy is included.

2.2. Statistical Ensembles and Related Algorithms. Periodic boundary conditions were implemented with the minimum image convention.[36] Dispersion and repulsion interactions were evaluated with a spherical cutoff radius equal to half of the simulation box length, associated with standard long-range corrections. In the case of the OPLS-AA model,[30] the electrostatic interaction energy was computed by using an Ewald summation with seven vectors in every dimension of the reciprocal space and a scaling parameter $\alpha = 0.3$ Å^{-1} in the direct space.

2.2.1. Phase Equilibria. The Gibbs ensemble Monte Carlo method[37] was used in order to compute phase equilibria. Although the benzene molecule is considered to be rigid in all of the models tested in this study, a statistical bias algorithm was used for molecular transfers between phases. This involved the selection of a suitable location for the center of mass in a first step and the test of several orientations in a second step.[20] The selected probabilities for the various types of moves were generally 0.3 for translations, 0.3 for rotations, 0.395 for transfers, and 0.005 for volume changes. Most simulations were carried out using a total of 220 molecules.

The molar vaporization enthalpy is computed as the difference between the average molar enthalpies of the liquid and those of the vapor simulation boxes. The statistical uncertainty on this property is typically 1−2%. The average liquid density was generally determined with a statistical uncertainty of 0.5−1%, but higher values (up to 5%) were found at near-critical temperatures as a result of the larger fluctuations. Once we have computed the vapor−liquid coexistence density curves, the critical temperature was obtained by fitting the critical scaling law $\rho_l - \rho_v = \lambda(T_c - T)^{0.325}$. The law of rectilinear diameters, $1/2(\rho_l + \rho_v) = \rho_c + \gamma(T - T_c)$, was then used to estimate the critical density.

2.2.2. Liquid Properties under Ambient Conditions. Simulations in the NpT isothermal−isobaric ensemble were performed on systems of 256 molecules to obtain the saturated liquid properties at 298 or 293 K. The molar enthalpy of vaporization is given by the following equation:

$$\Delta H_{vap} = -\langle E_{liq(\{int\}er)}\rangle + RT \tag{2}$$

where $\langle E_{vap(\{int\}er)}\rangle$ is the average molar intermolecular potential energy in the simulation. This relationship assumes that (i) the molar volume of the liquid is negligible compared with the vapor and (ii) the vapor is close enough to an ideal gas. These assumptions are correct for benzene at 298 or 293 K because the vapor pressure is significantly lower than atmospheric pressure. As liquid properties are not significantly different when pressure is set to either the experimental or to zero vapor pressure, the NpT simulations at 298 or 293 K have been made at zero pressure.

2.3. Optimization Method of Force Field Parameters. The following dimensionless error criterion was used:

$$F = \sum_{i=1}^{n} \frac{(X_i^{mod} - X_i^{exp})^2}{s_i^2} \tag{3}$$

where s_i is the estimated statistical uncertainty on the computed variable X_i^{mod}, estimated from a simulation using the standard block averaging technique,[36] while X_i^{exp} is the associated experimental measurement [either $\ln(P^{sat})$, ΔH_{vap}, or ρ_l]. F is taken to be a function of the potential parameters to optimize y_j. If every reference property is expanded as a first-order Taylor expansion, the minimization of F with respect to all y_j leads to the following condition:

$$\sum_{i=1}^{n} \frac{\left(X_i^{mod}(y^\circ) - X_i^{exp} + \sum_{k=1}^{3} \frac{\partial X_i^{mod}}{\partial y_k}\Delta y_k\right)\frac{\partial X_i^{mod}}{\partial y_j}}{s_i^2} \tag{4}$$

In this expression, the derivatives $\partial X_i^{mod}/\partial y_k$ have been evaluated by finite differences at the point y_j°. Once these derivatives are known, the Δy_k can be obtained by solving a linear system of equations.

3. AUA Parameter Optimization

The three AUA parameters that need to be optimized in the case of benzene for the CH group are the two Lennard−Jones parameters (ϵ and σ) and the offset distance δ (i.e., the distance

TABLE 1: Location of Force Centers and Intermolecular Potential Parameters of Benzene Models[a]

model	group	σ (Å)	ϵ/k (K)	α	Q (e)	B (Å)[b]	δ (Å)[c]
AUA (this work)	CH	3.2464	89.415			1.8071	0.4071
EW (*28*)	CH	3.5	77.0			1.756	0.346
FL (*29*)	CH	3.347	77.0			1.70	0.29
OPLS-AA (*30*)	C	3.55	35.225		−0.115	1.40	
	H	2.42	15.097		0.115	2.48	
Linse-UA (*32*)	CH	3.75	48.0			1.41	0
Claessens-UA (*27*)	CH	3.72	55.3			1.41	0
EP-UA (*15*)	CH	3.71	74.06	20		1.40	0
TraPPE-UA (*10*)	CH	3.695	50.5			1.40	0

[a] All models respect the planar hexagonal symmetry. [b] Distance between the center of the molecule and the interaction site. [c] Offset distance between the carbon center and the interaction site.

TABLE 2: Reference Data and Simulation Conditions Used for Optimization of AUA Potential Parameters of Benzene[a]

T (K)	simulation conditions	type of data	AUA this work	exptl data
450	GEMC	P^{sat} (kPa)	1001	973
		ΔH_{vap} (kJ/mol)	24.09	24.04
		ρ_l (kg/m^3)	690.7	692.7
293	monophasic, NpT, $P = 0$	ΔH_{vap} (kJ/mol)	34.08	34.1
		ρ_l (kg/m^3)	877.4	877.7

[a] Vapor pressure (P^{sat}), vaporization enthalpies (ΔH_{vap}), and liquid densities (ρ_l).

separating the carbon center from the force center as shown in Figure 1).

3.1. Reference Data. The first step in this optimization is to select a set of reference experimental data to be incorporated in the error criterion of eq 3. Three reference data are related to the equilibrium properties of benzene at 450 K: the vapor pressure, the vaporization enthalpy, and the liquid density (see Table 2). This temperature was selected because it allows an accurate determination of the equilibrium properties with the Gibbs ensemble technique. Two reference data are provided by the vaporization enthalpy and the saturated liquid density at 293 K, which can be conveniently evaluated by a NpT simulation at zero pressure. The experimental data have been taken from the interpolation formulas provided by the Dortmund Data Bank after having checked their reliability on reference measurements. Thus two simulations are sufficient to evaluate the five reference data included in the error criterion. The number of independent reference data is chosen to be larger than the number of parameters to be optimized so that there is a priori a high probability that they can be determined unambiguously.

3.2. Parameter Optimization. In the optimization procedure, it is important to select a suitable set of initial values y_j° (i.e., an initial parameter set that is close enough to the desired optimum to avoid divergence of the optimization process). For this purpose we used the set of AUA parameters representing the CH group of olefins,[21] which proved to be very efficient as a good optimum was found as soon as the first iteration.

In this first iteration, the average dimensionless error (i.e., the square root of eq 3) is greatly improved since it changes from $F^{1/2} = 8.43$ using the initial parameter set to $F^{1/2} = 0.56$ for the optimized set. The fact that the dimensionless error is significantly lower than unity means that the final deviations are smaller than the estimated statistical uncertainties on average. As a consequence, it would be meaningless to try a further optimization of the parameters unless more precise simulation methods are used.

The potential parameters from this optimization procedure are given in Table 1. The final values taken by the three parameters σ, ϵ, and δ in the proposed model are rather close

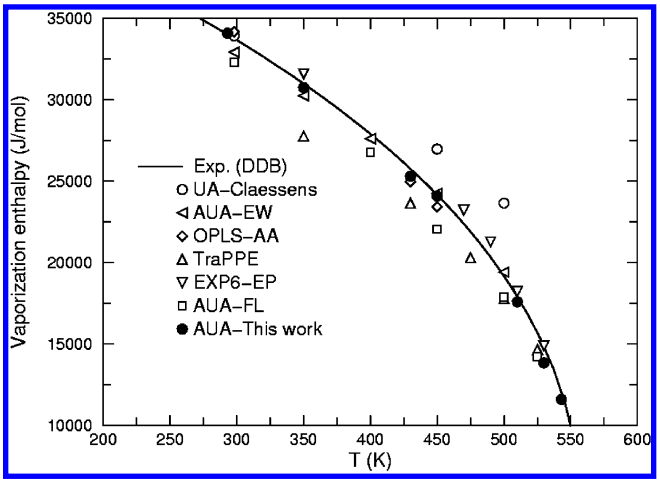

Figure 2. Vaporization enthalpy of benzene computed with the new potential (AUA-This work), the potential of Claessens et al.[27] (UA-Claessens), the potential of Evans and Watts[28] (AUA-EW), the potential of Jorgensen and Severance[30] (OPLS-AA), the potential of Wick et al.[10] (TraPPE), the potential of Errington and Panagiotopoulos[15] (EXP6-EP), and the potential of Friedrich and Lustig[29] (AUA-FL) compared with experimental data [correlation of the Dortmund Data Bank, version 2002].

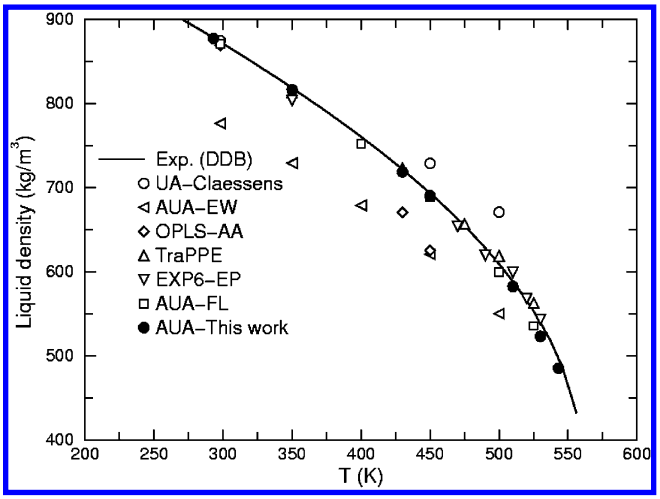

Figure 3. Saturated liquid density of benzene computed with the new potential (AUA-This work), the potential of Claessens et al.[27] (UA-Claessens), the potential of Evans and Watts[28] (AUA-EW), the potential of Jorgensen and Severance[30] (OPLS-AA), the potential of Wick et al.[10] (TraPPE), the potential of Errington and Panagiotopoulos[15] (EXP6-EP), and the potential of Friedrich and Lustig[29] (AUA-FL) compared with experimental data.

to the models using offset force centers (i.e., Friedrich−Lustig[29] and Evans−Watts[28]). They exhibit more important differences with the classical UA model,[10,27,32] which shows larger molecular diameters σ and smaller energy parameters ϵ. It is also interesting to note that the new potential parameter set is similar to those found previously for the olefinic CH group.[21]

4. Thermodynamic Properties

The vaporization enthalpy, saturated liquid density, and vapor pressure predicted by the new AUA potential and the various models are given in Table 3 and Figures 2−5. The estimation of the critical properties of the new AUA potential yields a critical temperature $T_c = 558$ K (i.e., 0.7% lower than the real value of 562.2 K). The estimated critical density is found to be $\rho_c = 302$ kg/m^3 (i.e., exactly equivalent to the experimental observations; see Figure 5). The normal boiling temperature obtained by interpolating the vapor pressure curve is $T_b =$

TABLE 3: Comparison of Predicted and Experimental Equilibrium Properties of Benzene with Various Intermolecular Potential Energy Models[a]

benzene model	T (K)	ensemble	property	calcd values	exptl values	% err	T (K)	ensemble	property	calcd values	exptl values	% err
Claessens et al.[27]	298	NpT	ΔH_{vap}	33.9	33.7	0.59	500	Gibbs	P^{sat}	1404	2160	−35.00
			ρ_l	874.9	873.2	0.19			ΔH_{vap}	23.7	19.2	23.44
	450	Gibbs	P^{sat}	635.6	968.9	−34.40			ρ_l	670.8	609.4	10.08
			ΔH_{vap}	26.9	24.1	11.62						
			ρ_l	728.9	693.5	5.10						
Evans−Watt[28]	298	NpT	ΔH_{vap}	32.92	33.7	−2.31	450	Gibbs	P^{sat}	942	969	−2.79
			ρ_l	776.3	873.2	−11.10			ΔH_{vap}	24.3	24.1	0.83
	350	Gibbs	P^{sat}	88.4	91.5	−3.39			ρ_l	620.8	693.5	−10.48
			ΔH_{vap}	30.45	30.9	−1.46	500	Gibbs	P^{sat}	2124	2160	−1.67
			ρ_l	729.4	818.7	−10.91			ΔH_{vap}	19.4	19.2	1.04
	400	Gibbs	P^{sat}	380	351.9	−3.38			ρ_l	550.5	609.4	−9.67
			ΔH_{vap}	27.6	27.9	−1.08						
			ρ_l	678.8	760.6	−10.75						
Errington Exp-6[15]	350	Gibbs	P^{sat}	91.3	91.5	−0.22	510	Gibbs	P^{sat}	2446	2491	−1.81
			ΔH_{vap}	31.6	30.9	2.27			ΔH_{vap}	18.2	17.9	1.68
			ρ_l	803.6	818.7	−1.84			ρ_l	594.4	588.8	0.95
	470	Gibbs	P^{sat}	1383	1385	−0.14	530	Gibbs	P^{sat}	3110	3265	−4.75
			ΔH_{vap}	23.8	22.3	6.73			ΔH_{vap}	14.9	14.8	0.68
			ρ_l	654.	662.7	−1.31			ρ_l	543.4	540.0	0.63
	490	Gibbs	P^{sat}	1849	1864	−0.80						
			ΔH_{vap}	21.8	20.3	7.39						
			ρ_l	619.9	628.4	−1.35						
OPLS-AA[30]	298	NpT	ΔH_{vap}	34.16	33.7	1.36	450	Gibbs	P^{sat}	475	969	−50.98
			ρ_l	869.1	873.2	−0.47			ΔH_{vap}	23.4	24.1	−2.90
	430	Gibbs	P^{sat}	336.8	666	−49.43			ρ_l	625.4	693.5	−9.82
			ΔH_{vap}	24.9	25.8	−3.49						
			ρ_l	670.6	721.7	−7.08						
TraPPE[10]	350	Gibbs	P^{sat}	123	91.5	34.43	500	Gibbs	P^{sat}	2568.0	2160.3	18.87
			ΔH_{vap}	27.7	30.9	−10.36			ΔH_{vap}	17.8	19.2	−7.29
			ρ_l	812.8	818.7	−0.72			ρ_l	618.8	609.4	1.54
	430	Gibbs	P^{sat}	866	666	30.03	525	Gibbs	P^{sat}	3428	3056	12.17
			ΔH_{vap}	23.6	25.8	−8.53			ΔH_{vap}	14.6	15.7	−7.01
			ρ_l	722.73	721.7	0.14			ρ_l	563.1	553.5	1.73
	475	Gibbs	P^{sat}	1749.4	1477.2	18.43						
			ΔH_{vap}	20.3	21.9	−7.31						
			ρ_l	657.1	654.5	0.40						
Friedrich−Lustig[29]	298	NpT	ΔH_{vap}	32.3	33.7	−4.15	500	Gibbs	ΔH_{vap}	17.9	19.2	−6.77
			ρ_l	871.1	873.2	−0.24			ρ_l	599.9	609.4	−1.56
	400	Gibbs	P^{sat}	408	351.9	15.94	525	Gibbs	P^{sat}	3600	3056	17.80
			ΔH_{vap}	26.8	27.9	−3.94			ΔH_{vap}	14.23	15.7	−9.36
			ρ_l	752.35	760.6	−1.08			ρ_l	535.7	553.5	−3.22
	450	Gibbs	P^{sat}	1233	969	27.24						
			ΔH_{vap}	22.1	24.1	−8.30						
			ρ_l	688.5	693.5	−0.72						
this work	293	NpT	ΔH_{vap}	34.08	34.1	−0.06	510	Gibbs	P^{sat}	2798	2491	12.32
			ρ_l	877.4	877.7	−0.03			ΔH_{vap}	17.59	17.92	−1.84
	350	Gibbs	P^{sat}	98.8	91.5	7.98			ρ_l	582.6	588.8	−1.05
			ΔH_{vap}	30.75	30.99	−0.77	530	Gibbs	P^{sat}	3480	3265	6.58
			ρ_l	816.6	818.7	−0.26			ΔH_{vap}	13.84	14.84	−6.74
	430	Gibbs	P^{sat}	740	666	11.11			ρ_l	523.5	540.0	−3.06
			ΔH_{vap}	25.1	25.8	−2.71	543	Gibbs	P^{sat}	4271	3858	10.71
			ρ_l	718.8	721.7	−0.40			ΔH_{vap}	11.6	12.1	−4.13
	450	Gibbs	P^{sat}	1001	973	2.88			ρ_l	485.64	498.2	−2.52
			ΔH_{vap}	24.09	24.04	0.21						
			ρ_l	690.7	692.7	−0.29						

[a] Vapor pressure (P^{sat}) is expressed in kPa, vaporization enthalpies (ΔH_{vap}) is in kJ/mol, and liquid density (ρ_l) in kg/m^3(Table 2).

350 K, compared with the actual value of 353.2 K. If we exclude the two highest temperatures, where phase properties are very sensitive due to the near-critical conditions, the average accuracy is approximately 0.5% on liquid density and 1% on vaporization enthalpy.

We start the comparison with the classical UA models (i.e., without offset) using the Lennard−Jones potential. The Claessens model[27] shows important deviations for all three properties at high temperature, and the Trappe model[10] seriously underestimates the vaporization enthalpy. Neither model provides a satisfactory representation of all three properties. The difficulty of classical UA models to match vaporization enthalpy has been already mentioned for *n*-alkanes.[18] It is likely that there are not enough degrees of freedom in this type of model to provide a detailed account of fluid phase behavior. On the other hand, the exponential-6 UA model[15] provides a very satisfactory prediction of vaporization enthalpy, liquid density, and vapor pressure over the whole range investigated (i.e., 350−530 K). The OPLS-AA model[30] correctly represents the liquid density and the vaporization enthalpy at 298 K but strongly underestimates the vaporization enthalpy and the vapor pressure at high temperature. Such a decreasing performance of the OPLS model at high temperature is not surprising as has already been noticed with organic sulfides and thiols, for instance.[22]

We finish this comparison with the AUA models. The Evans−Watts model[28] is found to strongly underestimate the

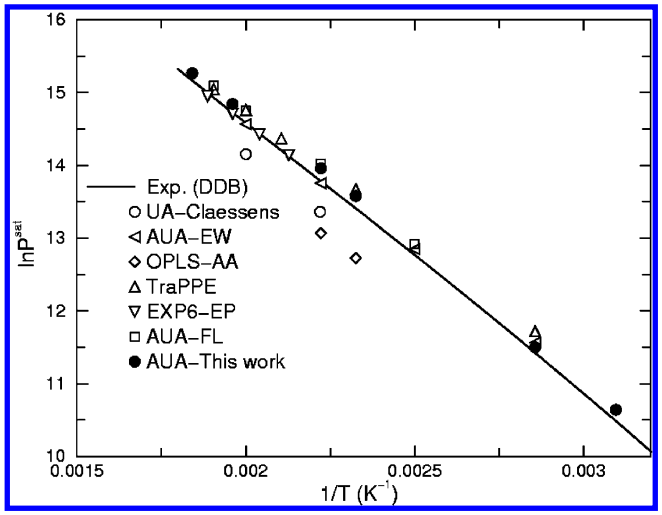

Figure 4. Vapor pressures of benzene computed with the new potential (AUA-This work), the potential of Claessens et al.[27] (UA-Claessens), the potential of Evans and Watts[28] (AUA-EW), the potential of Jorgensen and Severance[30] (OPLS-AA), the potential of Wick et al.[10] (TraPPE), the potential of Errington and Panagiotopoulos (*15*) (EXP6-EP), and the potential of Friedrich and Lustig[29] (AUA-FL) compared with experimental data.

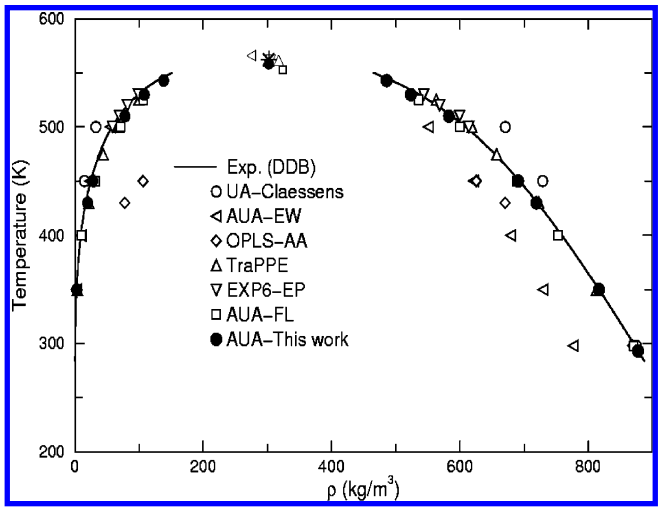

Figure 5. Vapor−liquid phase diagram computed with the seven models studied compared with the experimental coexistence curve. All symbols are equivalent to Figures 2−4. The experimental critical point is expressed with an asterisk, while the model critical points are expressed using the same symbol as for the coexistence densities.

liquid density. The Friedrich−Lustig model[29] however represents very well the observed trends, with the exception of a slight underestimation of vaporization enthalpies. Finally, the newly optimized AUA model from this work provides a satisfactory prediction of all properties. Only a slight overestimation of vapor pressure over the whole range investigated has been found. From this comparison, it may be concluded that the exponential-6 model[15] and the recent AUA potentials from this work and ref 29 are the most satisfactory, with deviations barely exceeding statistical uncertainties.

5. Structure of the Liquid Phase

The carbon−carbon intermolecular pair distribution function ($g_{CC}(r)$) of benzene is known from diffusion experiments,[38] and a comparison with simulation results is given in Figure 6. The appearance of the first shoulder at 3.8−4.5 Å is due to the closest possible approach of two carbon atoms, such as in parallel stacked dimers. The reason this shoulder is not a prominent

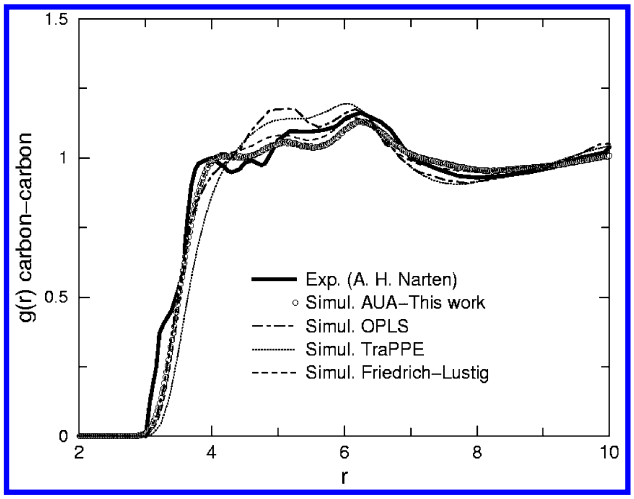

Figure 6. Carbon−carbon intermolecular pair distribution function for benzene computed with the new potential (AUA-This work), the potential of Jorgensen and Severance[30] (OPLS), the potential of Wick et al.[10] (TraPPE), and the potential of Friedrich and Lustig[29] (Friedrich−Lustig) compared with experimental data.

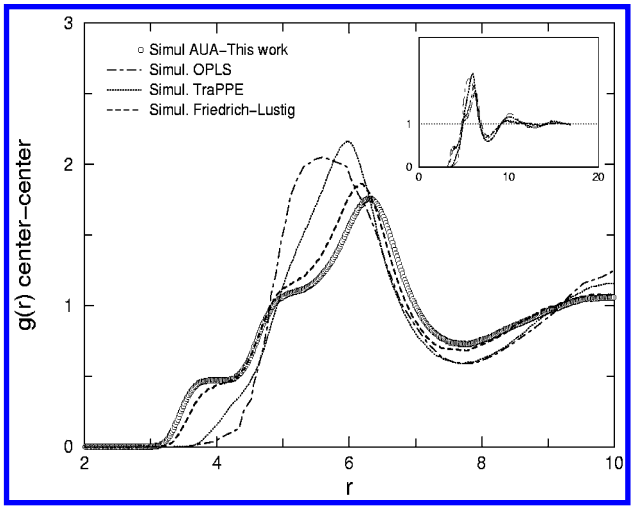

Figure 7. Center of mass pair distribution function for benzene computed with the new potential (AUA-This work), the potential of Jorgensen and Severance[30] (OPLS), the potential of Wick et al.[10] (TraPPE), and the potential of Friedrich and Lustig[29] (Friedrich−Lustig).

peak is attributed to the fact that the stacked configurations result in a significant electrostatic repulsion.[28,30,31] As a result, T-shaped conformations are significant, and the overall maximum of the carbon−carbon distribution function occurs for nonnearest neighbors at approximately 6 Å. The broad minimum around 8 Å corresponds to the depleted zone beyond the first shell of 12 benzene molecules. Despite their simplicity, the AUA potentials of Friedrich−Lustig[29] and of this study correctly describe the carbon−carbon distribution function. The TraPPE-UA model and the OPLS-AA model also represent the major features of this distribution but not as well as the AUA potentials.

The center of mass pair distribution function at ambient temperature, $g_{mm}(r)$, is shown in Figure 7. This distribution cannot be obtained directly from experimental data. The OPLS-AA model[30] exhibits a broad first maximum at 5.5 Å and a first minimum at 7.5 Å. A specific feature of the AUA models from the literature[28,29] and from this work is the presence of a shoulder at separation distances smaller than 4 Å. This close approach can be only explained by stacked parallel configurations. This feature is also found, although much less signifi-

cantly, with the TraPPE-UA model.[10] The absence of such shoulders in the OPLS model is due to the electrostatic repulsion in the stacked configurations. This can be compared with the structure of the solid phase of benzene, in which the nearest neighbor benzene molecules do not stack with their centers of mass on the symmetry axis.[25,26] It is therefore possible that the parallel stacking of benzene molecules with the AUA models is somewhat exaggerated. Another specific feature of the AUA models is the position of the main maximum at higher separation distances (6.1−6.5 Å) than the TraPPE-UA model (5.9 Å) and the OPLS-AA model (5.5 Å).

6. Conclusions

The new AUA potential developed on the basis of the thermodynamic properties of benzene (Table 2) provides a correct prediction of vaporization enthalpy, vapor pressure, and liquid density over a wide range of temperature from 293 to 543 K. The normal boiling point and the critical temperature are predicted with an accuracy better than 1%. The average accuracy is approximately 0.5% on liquid density and 1% on vaporization enthalpy. A detailed comparison with other models from the literature shows that the new AUA potential provides a better prediction of vapor−liquid equilibrium properties than the classical UA models tested,[10,27] the OPLS-AA model,[30] or the previous AUA model using different parameters.[28] Its results are equivalent to the exponential-6 UA model of Errington and Panagiotopoulos[15] and slightly better than the AUA model of Friedrich and Lustig.[29]

The liquid structure of benzene, as revealed by the carbon−carbon intermolecular pair distribution function, is also very well represented by the new AUA model. However the center−center radial pair distribution function shows a shoulder at separation distances lower than 4 Å that could be exaggerated. These results provide additional confirmation that the AUA potentials offer good accuracy and good physical relevance while still being remarkably simple. Further work is in progress to extend the AUA model to alkylaromatics, polyaromatics, and naphthenoaromatic hydrocarbons.

Acknowledgment. This work has been supported by the Ministerio de Ciencia y Tecnología of the Spanish Government (PPQ2000-2888E and PPQ2001-0671) and the Generalitat de Catalunya (2000ACI-13, 2001ACI-39, and ACI2002-37). R.O.C.-C. would like to thank the University Rovira i Virgili for financial support.

References and Notes

(1) Jorgensen, W. L.; Madura, J. D. *J. Am. Chem. Soc.* **1984**, *106*, 6638.
(2) Jorgensen, W. L.; Maxwell, D. S.; Tirado-Rives, J. *J. Am. Chem. Soc.* **1996**, *118*, 11225.
(3) Cornell, W. D.; Cieplak, P.; et al. *J. Am. Chem. Soc.* **1995**, *117*, 5179.
(4) Smit, B.; Karaborni, S.; Siepmann, J. I. *J. Chem. Phys.* **1995**, *102*, 2126..
(5) Sun, H. *J. Phys. Chem. B* **1998**, *102*, 7338−7364.
(6) Martin, M. G.; Siepmann, J. I. *J. Phys. Chem. B* **1998**, *102*, 2569.
(7) Martin, M. G.; Siepmann, J. I. *J. Phys. Chem. B* **1999**, *103*, 4508.
(8) Chen, B.; Siepmann, J. I. *J. Phys. Chem.* **1999**, *103*, 5370−5379.
(9) Chen, B.; Potoff, J. J.; Siepmann, J. I. *J. Phys. Chem. B* **2001**, *105*, 3093.
(10) Wick, C. D.; Martin, M. G.; Siepmann, J. I. *J. Phys. Chem. B* **2000**, *104*, 8008.
(11) Nath, S. A.; Escobedo, F. A.; de Pablo, J. J. *J. Chem. Phys.* **1998**, *108*, 9905.
(12) Nath, S. K.; Banaszak, B. J.; de Pablo, J. J. *J. Chem. Phys.* **2001**, *114*, 3612.
(13) Nath, S. K.; de Pablo, J. J. *Mol. Phys.* **2000**, *98*, 231−238.
(14) Errington, J. R.; Panagiotopoulos, A. Z. *J. Phys. Chem. B* **1999**, *103*, 6314.
(15) Errington, J. R.; Panagiotopoulos, A. Z. *J. Chem. Phys.* **1999**, *111*, 9731.
(16) Toxvaerd, S. *J. Chem. Phys.* **1990**, *93*, 4290.
(17) Toxvaerd, S. *J. Chem. Phys.* **1997**, *107*, 5197.
(18) Ungerer, P.; Beauvais, C.; Delhommelle, J.; Boutin, A.; Rousseau, B.; A. Fuchs, H. *J. Chem. Phys.* **2000**, *112*, 5499−5510.
(19) Bourasseau, E.; Ungerer, P.; Boutin, A.; Fuchs, A. H. *Mol. Simul.* **2002**, *28*, 317−336.
(20) Bourasseau, E.; Ungerer, P.; Boutin, A. *J. Phys. Chem. B* **2002**, *106*, 5483.
(21) Bourasseau, E.; Haboudou, M.; Boutin, A.; Fuchs, A. H.; Ungerer, P. *J. Chem. Phys.* **2003**, *118*, 3020.
(22) Delhommelle, J.; Tschirwitz, C.; Ungerer, P.; Granucci, G.; Millié, P.; Pattou, D.; A. Fuchs, H. *J. Phys. Chem. B* **2000**, *104*, 4745−4753.
(23) Kranias, S.; Pattou, D.; Levy, B.; Boutin, A. *Phys. Chem. Chem. Phys.* **2003**, *5*, 4175.
(24) Hadj-Kali, M.; Gerbaud, V.; Joulia, X.; Lagache, M.; Boutin, A.; Ungerer, P.; Mijoule, C.; Dufaure, C. *Chem. Eng. Trans.* **2003**, *3*, 1399.
(25) Bartell, L. S.; Sharkey, L. R.; Shi, X. *J. Am. Chem. Soc.* **1988**, *110*, 7006.
(26) Chelli, R.; Cardini, G.; Procacci, P.; Righini, R.; Califano, S. *J. Chem. Phys.* **2000**, *113*, 6851.
(27) Claessens, M.; Ferrario, M.; Ryckaert, J.-P. *Mol. Phys.* **1983**, *50*, 217.
(28) Evans, D. J.; Watts, R. O. *Mol. Phys.* **1976**, *32*, 93.
(29) Friedrich, A.; Lustig, R. *J. Mol. Liq.* **2002**, *98*−*99*, 241.
(30) Jorgensen, W. L.; Severance, D. L. *J. Am. Chem. Soc.* **1990**, *112*, 4768.
(31) Karlström, G.; Linse, P.; Wallqvist, A.; Jönsson, B. *J. Am. Chem. Soc.* **1983**, *105*, 3777.
(32) Linse, P. *J. Am. Chem. Soc.* **1984**, *106*, 5425.
(33) Smith, G. D.; Jaffe, R. L. *J. Phys. Chem.* **1996**, *100*, 9624.
(34) Tassing, T.; Cabaço, M. I.; Danten, T.; Besnard, M. *J. Chem. Phys.* **2000**, *113*, 3757.
(35) Friedrich, A.; Lustig, R. *J. Chem. Phys.* **1996**, *105*, 9597.
(36) Allen, M. P.; Tildesley, D. J. *Computer Simulation of Liquids*; Oxford Science Publications: Oxford, 1987.
(37) Panagiotopoulos, A. Z. *Mol. Phys.* **1987**, *61*, 813−826.
(38) Narten, A. H. *J. Chem. Phys.* **1977**, *67*, 2102.